

1 New turtle remains from the Late Cretaceous of Monte Alto-SP, Brazil, including cranial osteology,
2 neuroanatomy and phylogenetic position of a new taxon

3

4 Gabriel S. Ferreira,^{1,2,3*} Fabiano V. Iori,^{4,5} Guilherme Hermanson^{1,6} and Max C. Langer¹

5

6 ¹Laboratório de Paleontologia de Ribeirão Preto, Faculdade de Filosofia, Ciências e Letras de Ribeirão
7 Preto, Universidade de São Paulo, Avenida Bandeirantes 3900, 14040-901, Ribeirão Preto, SP, Brazil

8 ²Senckenberg Center for Human Evolution and Palaeoenvironment (HEP) at Eberhard Karls Universität,
9 Sigwartstraße 10, 72076 Tübingen, Germany

10 ³Fachbereich Geowissenschaften der Eberhard Karls Universität Tübingen, Hölderlinstraße 12, 72074
11 Tübingen, Germany

12 ⁴Museu de Paleontologia “Prof. Antonio Celso de Arruda Campos”, Centro de Artes, Praça do Centenário,
13 15910-000, Monte Alto, SP, Brazil

14 ⁵Museu de Paleontologia “Pedro Candolo”, Estação Cultura, Praça Farmacêutico Bruno Garisto, 15890-
15 000, Uchoa, SP, Brazil

16 ⁶Department of Earth Sciences, University of Oxford, South Parks Road, Oxford OX1 3AN, UK

17 *Corresponding author: +55 16 3315 4984; gsferreirabio@gmail.com

18

19 ORCID: GSF: 0000-0003-1554-8346; GH: 0000-0002-6917-1938; MCL: 0000-0003-1009-4605

20

21 **Abstract:** A high diversity of land vertebrates is known from the Late Cretaceous deposits of the Bauru
22 Basin, Brazil, including at least five turtle taxa, all belonging to the clade Podocnemidoidea. Some of the
23 richest fossil sites of this basin are in the area of Monte Alto, which yielded several squamate, dinosaur,
24 and crocodyliform taxa. Yet, the single turtle reported so far from this area was only briefly described.
25 Here, we further describe that specimen, a complete but very crushed shell, as well as a partial skull, both
26 found in outcrops of the Adamantina Formation. Comparison of the shell to other podocnemidoid taxa
27 reveals its affinities to *Roxochelys wanderleyi*, a turtle originally described from that same stratigraphic
28 unit. The comparative description of the skull and its inclusion in a phylogenetic study, supports the
29 proposal of a new taxon representing a lineage (*Peiropemydodda*) so far known only from the Marília
30 Formation of the Bauru Basin and the early Paleocene of Bolivia. The digitally reconstructed endocast
31 and inner ear of the new taxon were also described, as not previously done for a fossil pleurodire.

32

33 **Keywords:** Podocnemidoidea; Pleurodira; inner ear; neuroanatomy; carotid circulation; Late Cretaceous
34 Brazil; Adamantina Formation

35

36 **Acknowledgments**

37 We thank A. C. Arruda-Campos (in memoriam) for providing the material for study, L.E. Sabino (from
38 the FOAr-UNESP), for the microCT scanning, T. S. Fachini for sharing information about the fossil
39 vertebrate record of the Monte Alto region, and the crew involved in field activities, in particular C. A.
40 Francisco, D. Silva, and T. S. Fachini. We also acknowledge the reviewers, W.G. Joyce and I. Danilov,
41 and M. Reich for insightful comments that improved very much the manuscript, and E. Cadena and P.S.R.
42 Romano for useful suggestions on an earlier version of it. This work was supported by Fundação de
43 Amparo à Pesquisa do Estado de São Paulo (FAPESP) scholarships to GSF [grants number 2014/25379-5
44 and 2016/03934-2] and GH [grant number 2016/03373-0 and 2016/17116-0], and research funding to
45 MCL [2014/03825-3].

46

47

48 **Introduction**

49

50 The Late Cretaceous deposits of the Bauru Basin have yielded a high diversity of land vertebrates,
51 including anurans, lizards, crocodylomorphs, non-avian and avian dinosaurs, and mammals (e.g., Bertini
52 et al. 1993; Alvarenga and Nava 2005; Brito et al. 2006; Bittencourt and Langer 2011; Martinelli and
53 Nava 2011; Báez et al. 2012). The record of freshwater turtles is also rich, including five valid taxa,
54 namely *Bauruemys elegans* (Suárez, 1969), *Cambaremys langertoni* França and Langer, 2005,
55 *Peiropemys mezzalirai* Gaffney et al., 2011, *Pricemys caiera* Gaffney et al., 2011, and *Roxochelys*
56 *wanderleyi* Price, 1953, two dubious taxa, “*Podocnemis*” *harrisi* Pacheco, 1913, and “*Podocnemis*”
57 *brasiliensis* Staesche, 1937, and more fragmentary records that may represent additional taxa (e.g.,
58 Gaffney et al. 2011; Kischlat 2015; Menegazzo et al. 2015; Hermanson et al. 2016; but see Romano et al.
59 2013 for other taxonomic interpretations). All Bauru group turtles belong to the stem-based clade
60 Podocnemidoidae (França and Langer 2006; Podocnemididae of Gaffney et al. 2011), a side-necked turtle
61 lineage that includes the crown-group Podocnemididae and its sister-clade Peiropemydodda (see
62 Phylogenetic Definition and Comments below).

63 Deposits of the Adamantina and Marília formations crop out extensively in the area of Monte
64 Alto, São Paulo, Brazil, and their study has been chief to improve the knowledge of the vertebrate fauna
65 of the Bauru Basin. The fossil record in the region includes notosuchian (Pinheiro et al. 2008; Andrade
66 and Bertini 2008; Iori and Carvalho 2009, 2011), peirosaurid (Carvalho et al. 2007), and trematochampsid
67 crocodyliforms (Iori and Garcia 2012), titanosaur (Bertini et al. 2001; Santucci and Arruda-Campos 2011)
68 and theropod dinosaurs (Mendez et al. 2014; Tavares et al. 2014), as well as squamates (Fachini and Iori
69 2009; Fachini and Hsiou 2011). A single turtle specimen from the area, assigned to Pleurodira, has been
70 briefly reported in a conference abstract (Iori and Carvalho 2010).

71 Here, we present additional turtle specimens from the Late Cretaceous deposits of Monte Alto.
72 One of those, an almost complete skull, represents a new podocnemidoid taxon, *The new taxon*. Its
73 osteology and neuroanatomy is described here and the taxon is included in a phylogenetic analysis.
74 Additionally, we further describe the material previously reported by Iori and Carvalho (2010), also
75 presenting new specimens collected in the same region.

76

77

78 **Geological Settings and material**

79 The Bauru Basin (Fig. 1) is a large depression developed during the Cretaceous in the southeastern
80 portion of the South American Plate (Fernandes and Coimbra 1996). The filling-up of this basin occurred
81 under semi-arid to arid climatic conditions, between the Aptian and the Maastrichtian (Batezelli 2015).
82 Two of its lithostratigraphic units crop out in the area of Monte Alto-SP, the Adamantina and Marília
83 formations. Although the the stratigraphy and age of the Bauru Basin units are controversial, there is a
84 broad consensus that the Adamantina Fm. is older than the Marília Fm. (for a recent review on the issue,
85 see Menegazzo et al. 2016).

86 The specimens described here were collected from two different sites in the area of Monte Alto
87 that yield the sandy fluvial/lacustrine deposits of the Adamantina Formation (Fernandes and Coimbra
88 1994, 1996; Dias-Brito et al. 2001; Batezelli et al. 2003, 2005). MPMA 04-0008/89 comes from the
89 “Barreiro” site, along road SP-333, at the entrance to “Sítio da Serra”, type-locality of the crocodyliform
90 *Barreirosuchus franciscoi* (Iori and Garcia 2012). This site exposes an approximately 50 m thick
91 sequence, composed mostly of the Adamantina Formation topped by the Marília Formation. The
92 specimen described herein, along with bivalve, fish, crocodyliform, and sauropod dinosaur remains were
93 recovered from the basal bed (Iori and Garcia 2012), mostly composed of lightly cemented fine reddish
94 sandstones, with sparse carbonate nodules. In the same bed, disarticulated post-cranial remains of at least
95 three other turtles were also found (MPMA 04-0009/89, MPMA 04-0014/89 and MPMA 04-0017/89).
96 The turtle skeletons disarticulated during the biostratigraphic phase, but remained concentrated in the same
97 area.

98 The other specimen described here (MPMA 10-0003/03) was found in a small isolated outcrop
99 of the Adamantina Formation (S 21° 14' 03,6 ", W 48° 30' 27,5 ") in a farm near the urban area of Monte
100 Alto. The bearing rock corresponds to a strongly cemented fine reddish sandstone, with sparse pebbles
101 and carbonate nodules found near the turtle shell. The remains are partially articulated, with numerous
102 cracks formed by the diagenetic processes.

103 **Institutional Abbreviations** AMNH, American Museum of Natural History, New York, USA;
104 CPPLIP, Centro de Pesquisas Paleontológicas “Llewellyn Ivor Price”, Peirópolis, Uberaba, Brazil; MCT
105 (DGM), Museu de Ciências da Terra, Divisão de Geologia e Mineralogia, Departamento Nacional de
106 Produção Mineral, Rio de Janeiro, Brazil; MCZ, Museum of Comparative Zoology, Harvard University,
107 Cambridge, Massachusetts, USA; MN, Museu Nacional, Universidade Federal do Rio de Janeiro, Brazil;

108 **MPMA**, Museu de Paleontologia “Prof. Antonio Celso de Arruda Campos”, Monte Alto, Brazil;
109 **LPRP/USP**, Laboratório de Paleontologia de Ribeirão Preto, University of São Paulo, Ribeirão Preto,
110 Brazil.

111 **Anatomical Abbreviations ii and vii**, epidermal scutes (sensu Ferreira et al. 2015); **a.a.**, anterior
112 ampulla; **ap**, antrum postoticum; **asc**, anterior semicircular canal; **bo**, basioccipital; **bs**, basisphenoid; **cc**,
113 cavum cranii; **ccv**, canalis cavernosus; **ce.c**, cerebral branch of internal carotid; **cer**, cerebral hemisphere;
114 **cm**, condylus mandibularis; **cnv**, canalis nervi vidiani; **co**, costal plates; **col**, columella auris; **col.f**,
115 columella auris footplate; **cpt**, cavum pterygoidei; **cr**, cartilaginous ridge; **cru**, crus communis; **ct**,
116 canalis stapedio-temporalis; **ct**, cavum tympani; **ent**, entoplastron; **epi**, epiplastron; **ex**, exoccipital; **facci**,
117 foramen anterius canalis caroticus interni; **fel**, foramen caroticus laterale; **fjp**, foramen jugulare posterius;
118 **fm**, foramen magnum; **fnt**, foramen nervi trigemini; **fnv**, foramen nervi vidiani; **fo**, fenestra ovalis; **fpc**,
119 fossa precolumellaris; **fpo**, fenestra postotica; **fpp**, foramen palatinum-posterius; **fr**, frontal; **hyo**,
120 hyoplastron; **hyp**, hypoplastron;; **ica**, incisura columella auris; **ie**, inner ear; **ju**, jugal; **lag**, lagena; **lsc**,
121 lateral semicircular canal; **ma**, marginal scute; **me**, mesoplastron; **med**, medulla oblongata; **mx**, maxilla;
122 **ne**, neural plates; **nu**, nuchal plates; **op**, opisthotic; **och**, otic chamber; **ofb**, olfactory bulb; **oft**, olfactory
123 tract; **pa**, parietal; **p.a**, posterior ampulla; **pa.c**, palatal branch of internal carotid; **pal**, palatine; **pe**,
124 peripheral plates; **pf**, prefrontal; **pit**, pituitary fossa; **pm**, premaxilla; **po**, postorbital; **psc**, posterior
125 semicircular canal; **pt**, pterygoid; **ptp**, processus trochlearis pterygoidei; **qj**, quadratojugal; **qu**, quadrate;
126 **rbs**, rostrum basisphenoidale; **scv**, sulcus cavernosus; **so**, supraoccipital; **sot**, septum orbitotemporale;
127 **spp**, sulcus palatino-ptyerygoideus; **st**, sella turcica; **V**, trigeminal nerve; **VI**, abducens nerve; **VII**, facialis
128 nerve; **VII.p**, palatine (or vidian) branch of VII; **ve**, vertebral scute; **xip**, xiphoplastron.

129

130 **Methods**

131

132 A phylogenetic data-matrix with 39 taxa and 95 characters (see Nexus file in the Supplementary Data)
133 was compiled using the original matrix of Gaffney et al. (2011), with the addition of MPMA 04-0008/89,
134 *Bairdemys thalassica* (Ferreira et al. 2015), and 21 characters from other sources (see Supplementary
135 Data; Gaffney et al. 2006; Meylan et al. 2009; Cadena et al. 2012; Dumont Junior 2013; Cadena 2015;
136 Ferreira et al. 2015). As MPMA 04-0008/89 is clearly a representative of the Podocnemidoidae, based on
137 the presence of the processus trochlearis pterygoidei and cavum pterygoidei, we chose to use this data-

138 matrix that focuses on this lineage, instead of more inclusive ones (e.g. Gaffney et al. 2006; Cadena
139 2015). The matrix was analyzed in TNT v. 1.5 (Goloboff et al. 2008), with Chelidae set as the primary
140 outgroup and parsimony as the search criterion (“traditional search” with 1.000 replicates, hold 20,
141 random seed = 0, collapse of zero length branches). Functions implemented in TNT were employed to
142 summarize the most parsimonious trees (MPTs) in strict consensus, as well as to calculate Bremer support
143 and Bootstrap (GC, 1000 replicates; Goloboff et al. 2003) values.

144 Micro CT-scan images were obtained using a SkyScan 1176 at Faculdade de Odontologia de
145 Araraquara (FOAr-UNESP), with 721 projections over 360°, exposure time of 540 ms, voltage of 90 kV,
146 current of 275 µA, and a resolution of 17 µm per pixel. NRecon v. 1.6.9.8 and DataViewer v. 1.5.0 were
147 used to process the cross-sectional images. Materialise Mimics Research edition version 18.0 was used
148 for digital reconstructions and measurements of the skull bones and endocasts of the brain and inner ear.

149

150 **Systematic palaeontology**

151

152 **Pleurodira** Cope, 1864

153 **Pelomedusoides** Broin, 1988

154 **Peiopemydodda** Gaffney, Meylan, Wood, Simons and Campos, 2011

155 *Phylogenetic Definition.* Peiopemydodda refers to the branch-based clade that includes all taxa more
156 closely related to *Peiopemys mezzalirai* Gaffney et al., 2011, and *Lapparentemys vilavilensis* (Broin,
157 1971) than to *Podocnemis expansa* (Schweigger, 1812).

158

159 *gen. et sp. nov.*

160 *Diagnosis.* A small Podocnemidoidae based on the right angle formed by the processus trochlearis
161 pterygoidei and the cavum pterygoidei; a Peiopemydodda based on the anteroventral emargination
162 projecting above the ventral level of the orbit (Gaffney et al. 2011). Compared to other peiopemydod and
163 Bauru Group turtles, it is similar in size to *Bauruemys elegans*, but smaller than all other peiopemydods;
164 the skull is roughly the same height along its entire length, as in *Peiopemys mezzalirai* and
165 *Lapparentemys vilavilensis*, differing from that of *Bauruemys elegans*; the rostral tip of the basisphenoid
166 is acute as in *Pricemys caiera*, but not in *Bauruemys elegans* and *Peiopemys mezzalirai*; the foramen
167 palatinum posterius is formed by the palatine and pterygoid, differing from *Peiopemys mezzalirai*; the

168 fossa precolumellaris is very large as in *Peiropemys mezzalirai*, in contrast to *Pricemys caiera*; skull
169 dermal scute vii (sensu Ferreira et al., 2015; same as interparietal scute) has the anterior margins on the
170 frontal and lateral edges converging posteriorly as in *Bauruemys elegans*, *Lapparentemys vilavilensis* and
171 *Peiropemys mezzalirai*, but differing from the latter two by an anterior notch on the midline, as also found
172 in *Bauruemys elegans*.

173 *Material.* MPMA 04-0008/89 (Figs. 2-6), a partial skull lacking both premaxillae and squamosals, most
174 of the maxillae, and portions of several other bones (see Comparative Description) housed at the Museu
175 de Paleontologia “Prof. Antonio Celso de Arruda Campos”, Monte Alto, Brazil.

176 *Stratum and locality.* Reddish sandstones of the Late Cretaceous Adamantina Formation, exposed at the
177 entrance to “Sítio da Serra” (S 21° 15' 06.9”, W 48° 33' 10.4”), Monte Alto-SP, Brazil.

178 *Description.* The skull of MPMA 04-0008/89 is 35 mm long as preserved, much smaller than other
179 peiropemydods (e.g. the holotype of *Peiropemys mezzalirai* is approximately 90 mm long excluding the
180 crista supraoccipitalis, and the specimen AMNH 14444 referred to *Lapparentemys vilavilensis* is 96 mm
181 long). The adductor chamber is completely filled by matrix, but parts of its roof were imprinted in the
182 sandstone, forming a natural endocast (Fig. 2). The skull is relatively high at the orbital region, with a
183 value of 0.80 for the height at orbit/largest height ratio, approaching the condition of *Lapparentemys*
184 *vilavilensis* (AMNH 14444) and *Peiropemys mezzalirai* (MCT 147), which have 0.69 and 0.79 ratios,
185 respectively, whereas that of *Bauruemys elegans* (Kischlat and Azevedo 1991) ranges from 0.50 (MCZ
186 4123) to 0.55 (MCT 1753). Some epidermal scute sulci are poorly preserved, but various features can be
187 observed: based on the preserved borders, scute vii (sensu Ferreira et al. 2015) possibly formed a small
188 and equilateral triangle with smooth edges similar to that of *Peiropemys mezzalirai* and *Lapparentemys*
189 *vilavilensis*, but the anterior sulcus shared with scute ii on the frontal and postorbital has an anterior notch
190 on the midline, as in *Bauruemys elegans* (Gaffney et al. 2011); part of the posterior edge of scute ii is
191 preserved on the postorbital, but its extension cannot be determined.

192 **Prefrontal**

193 The prefrontal is partially preserved and it is therefore possible to identify its posterior contact with the
194 frontal. The bone forms the anteromedial edge of the orbit, as in most podocnemidoids. The interorbital
195 distance is similar to that of *Bauruemys elegans*, *Peiropemys mezzalirai*, and *Lapparentemys vilavilensis*
196 (Gaffney et al. 2011), and the large orbit is directed dorsolaterally as in other peiropemydods.

197 **Frontal**

198 As in most podocnemidoids, the frontal contacts the prefrontal anteriorly, the other frontal medially, the
199 postorbital posterolaterally, and the parietal posteriorly. It has an almost squared dorsal outline, with
200 subparallel lateral and medial edges, as in *Bauruemys elegans* and differing slightly from *Lapparentemys*
201 *villavilensis* and *Peiropemys mezzalirai*, which have diverging lateral and medial edges. The anterior and
202 posterior edges are also subparallel, as in *Peiropemys mezzalirai*, but not in *Hamadachelys escuilliei*,
203 *Lapparentemys villavilensis*, and most *Bauruemys elegans* specimens (although some have subparallel
204 edges, e.g., MCZ 4123 in Gaffney et al. 2011:fig. 13), in which the frontal-prefrontal suture projects
205 anteromedially. The frontal forms the anteromedial margin of the orbit, as in other podocnemidoids.

206 **Parietal**—Only the horizontal parietal plate is exposed in MPMA 04-0008/89 and its posterior margin is
207 not completely preserved (Fig. 2a). However, the limits of the posterodorsal emargination are preserved in
208 the natural cast of the adductor chamber, and it reached half the length of the cavum tympani, as in
209 *Bauruemys elegans* and *Pricemys caiera*, in contrast to the more extensive emargination of
210 *Hamadachelys escuilliei* and the less extensive ones of *Lapparentemys vilavilensis* and *Peiropemys*
211 *mezzalirai* (Tong and Buffetaut 1996; Gaffney et al. 2011). The parietal plate meets the frontal anteriorly,
212 the postorbital anterolaterally, the quadratojugal posterolaterally, and the other parietal medially, as seen
213 in other podocnemidoids (Gaffney et al. 2011). As in other peiropemydods, the medial suture between the
214 parietals extends posteriorly, and the supraoccipital either does not take part of the skull roof, or has only
215 a slight exposure on it (Gaffney et al. 2011). With the help of micro CT images (Fig. 3), it is possible to
216 identify the sutures of the processus inferior parietalis with the prootic posterolaterally, on the dorsal
217 surface of the otic chamber, the supraoccipital posteriorly, and the pterygoid anteriorly. As in most other
218 podocnemidoids, the parietal of MPMA 04-0008/89 forms the dorsal margin of the foramen nervi
219 trigemini (Fig. 3c), along with the prootic posteriorly and the pterygoid anteriorly (Gaffney et al. 2011).

220 **Jugal**

221 The jugal is fractured on both sides (Fig. 2) of MPMA 04-0008/89. Nevertheless, it is possible to identify
222 some of the contacts seen in most pelomedusoids: with the maxilla anteriorly, the postorbital dorsally, and
223 the quadratojugal posteriorly (Gaffney et al. 2006, 2011). Also, part of the ventral margin of the left jugal
224 is preserved and, together with the natural cast of the quadratojugal on the right side (Fig. 2c), allows
225 inferring the extension of the anteroventral emargination, which is composed by the jugal and

226 quadratojugal, as in other pelomedusoids (Gaffney et al. 2006, 2011). This emargination surpasses the
227 ventral level of the orbit dorsally (about half the height of the cavum tympani), as seen in *Peiropemys*
228 *mezzalirai* and *Lapparentemys vilavilensis*, and is likely synapomorphic of Peiropemydodda (unknown in
229 *Pricemys caiera*), differing from the less extensive anteroventral emarginations of *Hamadachelys*
230 *escuilliei* and *Bauruemys elegans*, which do not surpass the ventral margin of the orbit (Tong and
231 Buffetaut 1996; Gaffney et al. 2011).

232 **Quadratojugal**

233 The quadratojugal has preserved contacts with the postorbital anteromedially, the parietal medially, the
234 quadrate posterolaterally, and possibly the jugal anteriorly, as in other peiropemydods. The suture with the
235 squamosal is not preserved and that with the quadrate follows the anterior curvature of the cavum
236 tympani, as in other pelomedusoids (Gaffney et al. 2006, 2011). Compared to other non-Podocnemididae
237 podocnemidoids, the quadratojugal of *the new taxon* more similar to those of *Hamadachelys escuilliei*,
238 *Peiropemys mezzalirai* and *Lapparentemys vilavilensis*, differing from that of *Bauruemys elegans*, in
239 which it is antero-posteriorly compressed (Tong and Buffetaut 1996; Gaffney et al. 2011).

240 **Postorbital**

241 The postorbital is antero-posteriorly elongated, forming the posterodorsal margin of the orbit and
242 contacting the frontal medially, the parietal posteromedially, the quadratojugal posterolaterally, and the
243 jugal laterally (Fig. 2i, j). This differs from the very reduced postorbital of the different species of
244 *Podocnemis*, which is sometimes not even exposed in dorsal view (Gaffney et al. 2011). In *the new taxon*
245 it has a ventral projection that forms most of the septum orbitotemporale, contacting the jugal
246 ventrolaterally and the pterygoid ventrally at the anterior base of the processus trochlearis pterygoidei,
247 where it forms the posterodorsal part of the sulcus palatino-pterygoideus roof (Fig. 3b, c), as in other
248 pelomedusoids (Gaffney et al. 2011). In the anterior part of the septum orbitotemporale, the postorbital
249 contacts the frontal dorsomedially, the jugal ventrolaterally, and the palatine ventromedially (Fig. 3b, c).

250 **Maxilla**

251 Only small fragments of the right maxilla are preserved in MPMA 04-0008/89. It is possible to identify its
252 contact to the jugal posterodorsally and to the palatine posteroventrally (Fig. 2c).

253 **Palatine**

254 The anterior portion of the palatine is not preserved and only the posterior part of the horizontal
255 plate is exposed in MPMA 04-0008/89, with the vertical structures covered by matrix. It contacts the
256 maxilla anterolaterally, its counterpart medially, and the pterygoid posteriorly. The palatine appears to be
257 exposed on the orbital floor (Fig. 2a), covering the medial part of the maxilla, as typical of non-
258 Podocnemididae Podocnemidoidae, but not very clear in *Peiropemys mezzalirai*. The foramen palatinum
259 posterius reaches the palatine-ptyerygoid suture (Fig. 2e, 3a) as in *Lapparentemys vilavilensis* and some
260 specimens of *Bauruemys elegans*, differing from *Peiropemys mezzalirai*, in which it is restricted to the
261 palatine (Gaffney et al. 2011). The position of this foramen, however, may be variable within the same
262 taxon, as is the case in *B. elegans* (Gaffney et al. 2011).

263 **Quadrate**

264 As in other pleurodires, the quadrate of *the new taxon* forms the entire cavum tympani (Gaffney 1979;
265 Gaffney et al. 2006, 2011), contacting the lateral surface of the quadratojugal anteriorly. On the roof of
266 the otic chamber, the quadrate contacts the prootic anteriorly and the opisthotic posteromedially (Fig. 3a,
267 c). The fossa precolumellaris is very large, as in *Peiropemys mezzalirai*, and larger than those of other
268 non-podocnemidid podocnemidoids (Tong and Buffetaut 1996; Lapparent de Broin 2000; Gaffney et al.
269 2011). The antrum postoticum is also well-developed (Fig. 2k, l), comparable in size to those of
270 *Podocnemis unifilis* and *Galianemys emringeri* (Gaffney et al. 2006, 2011). The incisura columellae auris
271 is completely closed by the contact of the dorsal and ventral processes of the quadrate, as in other
272 Podocnemidoidae (Gaffney et al. 2011).

273 As in other pelomedusoids, the ventral surface of the quadrate of *the new taxon* meets the
274 basioccipital posteromedially and the basisphenoid medially, its anteromedial projection contacting the
275 pterygoid (Fig. 2e, f). It also forms part of the roof of the cavum pterygoidei, where it contacts the
276 pterygoid anterolaterally, the prootic anteromedially, and the basisphenoid posteromedially, as typical of
277 podocnemidoids (Lapparent de Broin 2000; Gaffney et al. 2011). Although the condylus mandibularis is
278 not preserved in MPMA 04-0008/89, it is possible to infer that it was anterior to the basisphenoid-
279 basioccipital suture, as in all other known podocnemidoids, except for some Stereogenyina (Gaffney et al.
280 2011; Ferreira et al. 2015). Very little is preserved of the posterior surface of the quadrate. Only an outline
281 of the fenestra postotica is seen (Fig. 2k), which is wide as in other podocnemidoids, differing from the
282 slit-like fenestra of *Cearachelyini* (Gaffney et al. 2006).

283 **Pterygoid**

284 As in most podocnemidoids, the pterygoid of *the new taxon* contacts the palatine anteriorly, its
285 counterpart medially, the quadrate posterolaterally, and the basisphenoid posteromedially. As
286 synapomorphic for pleurodires, the pterygoid forms the processus trochlearis pterygoidei laterally, which
287 is nearly perpendicular to the midline in MPMA 04-0008/89. This latter condition is typical of Pan-
288 Podocnemididae, compared to Chelidae or Pelomedusidae (Gaffney et al. 2006, 2011). Yet, the angle
289 formed by the lateral margin of the process is almost 90°, as in *Podocnemis expansa*, *Portezueloemys*
290 *patagonica*, *Peltocephalus dumerilianus*, *Peiropemys mezzalirai*, and other podocnemidids (de la Fuente
291 2003; Gaffney et al. 2011; Cadena 2015), whereas that angle is more oblique in *Bauruemys elegans*,
292 *Lapparentemys vilavilensis*, *Hamadachelys escuilliei*, *Cearachelys placidoi*, and most bothremydids
293 (Tong and Buffetaut 1996; Lapparent de Broin 2000; Gaffney et al. 2011). The pterygoid of *the new taxon*
294 also forms a well-developed pterygoid flange, typical of Podocnemidoidae (França and Langer 2006),
295 developing a complete cavum pterygoidei (Fig. 2e, 3e). The thin plate that forms the floor of the cavum
296 pterygoidei is very fragile and usually broken in fossil specimens (Gaffney et al. 2011), but it is partially
297 preserved in MPMA 04-0008/89 (Fig. 2f).

298 The cavum pterygoidei is also formed by the basisphenoid, prootic, and quadrate, in addition to
299 the pterygoid, as in all podocnemidoids (Gaffney et al. 2011). Its anterior opening is large and
300 corresponds to the foramen caroticum laterale (Fig. 3d), which is enlarged in *The new taxon*, as in other
301 peiropemydids and *Podocnemis* spp. (Gaffney et al. 2011). The cavity is roofed by the prootic and,
302 hence, not continuous to the canalis cavernosus as in *Peltocephalus dumerilianus* and *Erymnochelys*
303 *madagascariensis* (Lapparent de Broin 2000; Gaffney et al. 2011). Anteriorly to the foramen cavernosum
304 formed by the prootic and the quadrate, the sulcus cavernosus extends on the dorsal surface of the
305 pterygoid, running laterally to the rostrum basisphenoidale (Fig. 3e). The foramen caroticum laterale also
306 opens in this sulcus (Gaffney 1979). Finally, the very small foramen nervi vidiani can be seen in the 3D
307 model as a perforation on the pterygoid inside the cavum pterygoidei as in other podocnemidoids
308 (Gaffney et al. 2011), lateral to the foramen caroticum laterale (Fig. 3d). The canal for this branch of the
309 facialis nerve (Gaffney 1979) could only be reconstructed partially; it extends anteriorly along the
310 pterygoid, but its anteriormost portion cannot be determined (Fig. 3e).

311 **Supraoccipital**

312 The supraoccipital is not exposed on the skull roof of MPMA 04-0008/89 (Fig. 2a, 3c). This matches the
313 condition of all known Peiropemydodda, the parietals of which cover almost the entire dorsal surface of
314 that bone, in contrast to other podocnemidoids such as *Bauruemys elegans* and the different species of
315 *Podocnemis* (Gaffney et al. 2011). Other parts of the supraoccipital of MPMA 04-0008/89 are covered by
316 matrix and can only be seen in the micro CT images (Fig. 3). The bone forms the dorsal edge of the
317 foramen magnum, contacting the exoccipitals posteroventrally, the prootic anterolaterally, the opisthotic
318 posterolaterally, and the parietals anterodorsally (Fig.3c).

319 **Exoccipital**

320 The exoccipital of MPMA 04-0008/89 contacts the supraoccipital dorsally, the opisthotic laterally, and the
321 basioccipital ventrally (Fig. 2k, l). The contact with the quadrate cannot be seen in this specimen, but the
322 exoccipitals form the lateral edges of the foramen magnum. The foramina nervi hypoglossi are not
323 preserved and the foramen jugulare posterius seems partially preserved on its right side (Fig. 2k), but it is
324 not clear if it is continuous with the fenestra postotica as in *Bauruemys elegans* and *Portezueloemys*
325 *patagonica* (de la Fuente 2003; Gaffney et al. 2011), or closed as in peiropemydods and podocnemidids
326 (Gaffney et al. 2011).

327 **Basioccipital**

328 In ventral view, the basioccipital of MPMA 04-0008/89 contacts the basisphenoid anteriorly and the
329 quadrate laterally (Fig. 2f). The posterior most portion of the bone is not preserved and the contacts with
330 the opisthotic and exoccipital are not clearly seen (Fig. 2k). Although not entirely preserved, the tubercula
331 basioccipitale are smoother than in *Bauruemys elegans* and the different species of *Podocnemis* and the
332 space between the tubercula appears to be wider than in those taxa (Gaffney et al. 2011), and more similar
333 to the condition found in *Lapparentemys vilavilensis* and *Peiropemys mezzalirai* (Fig. 2e, f). **Prootic**

334 Most of the prootic is covered by matrix in MPMA 04-0008/89, but the micro-CT scan images and our
335 3D reconstructions reveal its contacts and several structures (Fig. 3). As in all podocnemidoids, the
336 prootic is completely covered in ventral view by the pterygoid, except inside the cavum pterygoidei, in
337 which it forms the dorsomedial portion of its roof (Gaffney et al. 2011) and contacts the basisphenoid
338 medially, the quadrate laterally, and the pterygoid anterolaterally. On its dorsal portion it also contacts the
339 opisthotic posteriorly, the supraoccipital posteromedially, and the parietal anteromedially. Together with

340 the parietal and pterygoid, it forms the border of the foramen nervi trigemini, which opens laterally on the
341 fossa temporalis inferior, as in other pleurodires (Gaffney et al. 2006, 2011).

342 Due to the poor contrast between fossil and matrix some smaller structures are difficult to
343 identify in the micro-CT images. The foramen nervi facialis in the prootic inside the cavum pterygoidei,
344 as found in *Pricemys caiera*, *Peiropemys mezzalirai*, and other podocnemidoids (Gaffney et al. 2011)
345 could not be identified. On the other hand, the canalis cavernosum, between the prootic and quadrate, as
346 well as the canalis stapedio-temporalis, could be completely reconstructed. The former starts posteriorly,
347 in the fenestra postotica, and extends anteriorly to the foramen cavernosus, bordered by the prootic
348 medially and quadrate laterally, following on the pterygoid as the sulcus cavernosus. The canalis stapedio-
349 temporalis, branches from nearly half-way the length of the canalis cavernosus, carrying the arteria
350 stapediales to the foramen stapedio-temporalis (Gaffney 1979). The latter is also bordered by the prootic
351 and quadrate, opening dorsally on the external surface of the otic chamber on the fossa temporalis
352 superior, as in other podocnemidoids (Gaffney et al. 2011).

353 **Opisthotic**

354 Only small parts of the opisthotic of MPMA 04-0008/89 are visible, but its dorsal surface can be seen in
355 the micro-CT images (Fig. 3). It is possible to identify the contacts to the prootic anteriorly, supraoccipital
356 medially, exoccipital posteromedially, and quadrate laterally, as in other podocnemidoids (Tong and
357 Buffetaut 1996; Lapparent de Broin 2000; Gaffney et al. 2011).

358 **Basisphenoid**

359 The basisphenoid differs from that of most non-podocnemidid podocnemidoids (Suárez 1969; Tong and
360 Buffetaut 1996; Lapparent de Broin 2000), except for *Pricemys caiera*, in having an acute anterior tip
361 exposed in ventral view (Fig. 2e, f). This could be an ontogenetic variation, as the sutural contact between
362 the pterygoids could extend posteriorly to cover that tip in older specimens. As in other podocnemidoids,
363 the basisphenoid of *The new taxon* has a pentagonal shape (Fig. 2e). It contacts the pterygoids anteriorly
364 and, inside the cavum pterygoidei, a small ventral exposure of the prootic anterolaterally. It also contacts
365 the quadrate laterally and the basioccipital posteriorly. The latter suture is smoother than in *Bauruemys*
366 *elegans* (Suárez 1969) and similar to those of peiropemydids (Gaffney et al. 2011).

367 On the dorsal surface of the basisphenoid of *The new taxon*, as revealed by our 3D model (Fig.
368 3e), the rostrum basisphenoidale projects anteriorly over the dorsal surface of the pterygoids. Posteriorly,

369 the sella turcica is preserved on the midline and its posterolateral walls are pierced by the foramen
370 anterius canalis carotici interni, through which the internal carotid artery enters the cavum cranii (Gaffney
371 1979). The foramen nervi abducentis is smaller and opens slightly posterior to the foramen anterius
372 canalis carotici interni, also laterally on the basisphenoid and inside the cavum pterygoidei.

373 **Cranial endocast**

374 The brain endocast reconstructed for MPMA 04-0008/89 exhibits a tubular shape (Fig. 4a), as in other
375 known extinct and extant turtles (Zangerl 1960; Gaffney 1977; Wyneken 2001; Paulina-Carabajal et al.
376 2013, 2017; Mautner et al. 2017). The medulla oblongata is located slightly below the level of the
377 cerebral hemispheres, similar to the extant *Dermochelys coriacea*, *Malacochersus tornieri*, and
378 *Macrochelys temminckii*, as well as to the extinct *Corsochelys haliniches* (Hopson 1979; Paulina-
379 Carabajal et al. 2013; Mautner et al. 2017). Yet, in these taxa and in *The new taxon* the braincase elements
380 are found almost in the same horizontal plane (Fig. 4a), differing from the condition of other
381 podocnemidoid turtles such as *Bothremys cooki* and *Chedighaii barberi* (Hopson 1979; Gaffney et al.
382 2006), and some sea turtles (Wyneken 2001), in which the pontine and cephalic flexures of the brain
383 position the medulla oblongata well below the cerebral hemispheres (Hopson 1979). The latter are easily
384 discernible in MPMA 04-0008/89 and more laterally expanded than in *Plesiochelys etalloni*, as also seen
385 in *Bothremys cooki* and *Corsochelys haliniches* (Hopson 1979). The olfactory bulbs project laterally just
386 anterior to the cerebral hemispheres, and the endocast continues anteriorly forming the slender olfactory
387 tract (Fig. 4a, b). Projecting ventrally from the ventral surface of the endocast it is possible to identify the
388 pituitary cast, in which the pituitary gland is located (Fig. 4a).

389 Dorsal to the cerebellum, a subtle subtriangular area is found (Fig. 4a, b), corresponding to the
390 cartilaginous ridge (Paulina-Carabajal et al. 2013), or cartilaginous “rider” (Gaffney and Zangerl 1968;
391 Gaffney 1982).. Among extinct turtles, *Bothremys cooki*, *Corsochelys haliniches*, and the baenid
392 *Plesiobaena antiqua* (Hopson 1979; Gaffney 1982), as well as meiolaniids (Paulina-Carabajal et al. 2017)
393 seem to possess a more prominent version of this ridge, as in *The new taxon*, but not in *Plesiochelys*
394 *etalloni* (Paulina-Carabajal et al. 2013).

395 Only some of the cranial nerves could be reconstructed in MPMA 04-0008/89 (Fig. 4). The canal
396 for the trigeminal nerve (V) projects laterally from the endocast, posteroventrally to the cerebral
397 hemispheres and dorsally to the pituitary cast (Fig. 4a). The facialis nerve (VII) leaves the endocast more

398 posteriorly, just anterior to the endosseous labyrinth, and extends laterally inside the prootic, to the canalis
399 cavernosus (Fig. 4b, c). The latter, after branching off from the dorsal canalis stapedio-temporalis (Fig.
400 4a), extends anteromedially. As in peiropemydods and *Podocnemis* spp. (Gaffney et al. 2011), it turns into
401 the sulcus cavernosus after leaving the foramen cavernosum, where it communicates with the ventral
402 cavum pterygoidei (Fig. 4a). The canalis cavernosus contains the lateral head vein in pleurodires (Gaffney
403 1979), which runs anteriorly through the sulcus cavernosus, lateral to the rostrum basisphenoidale (Fig.
404 3e). The canal for the palatine (or vidian) branch of the facialis nerve (Gaffney 1979) could be partially
405 identified inside the pterygoid. It leaves the anterior wall of the cavum pterygoidei and extends anteriorly
406 (Fig. 3e, 4c). A small canal anteroventral to the nerve facialis could be identified in the micro-CT scan
407 images, and could correspond to the abducens nerve (VI), which runs anteriorly (Paulina-Carabajal et al.
408 2013).

409 Finally, the cerebral and palatine branches of the internal carotid leave the cavum pterygoidei
410 anteromedially and anteriorly, respectively (Fig. 4c), as in all peiropemydods and podocnemidids
411 (Gaffney et al. 2011). The cerebral artery enters the pituitary fossa on the basisphenoid, and the palatine
412 artery runs anteriorly to the sulcus cavernosus on the dorsal surface of the pterygoid (Fig. 3e, 4c). Thus,
413 the split between the two branches of the internal carotid artery occurs inside the cavum pterygoidei,
414 floored by the pterygoid flange, which extends ventrally to that split (Gaffney et al. 2011). As in all
415 crown-turtles, the split of the internal carotid artery is, therefore, floored by bone (Sterli et al. 2010;
416 Müller et al. 2011), but this occurs in an open space (i.e., inside the cavum pterygoidei), and not within its
417 own canal (the canalis carotici interni; Gaffney 1979). The patterns of carotid circulation are well
418 documented in cryptodires and stem-turtles (Albrecht 1976; Sterli et al. 2010; Müller et al. 2011; Rabi et
419 al. 2013), but descriptions of both extant and extinct pleurodires are still lacking

420 **Inner ear**

421 The digitally reconstructed inner ear of *The new taxon* shows a morphology that generally resembles that
422 of other turtles (Wever 1978; Walsh et al. 2009; Paulina-Carabajal et al. 2013, 2017): the semicircular
423 canals are dorsoventrally low, subequal in size, and their cross-section is sub-elliptical, with a globose
424 lagena (Fig. 4d).

425 The inner ear cast is 9.2 mm long. The anterior (ASC) and posterior (PSC) semicircular canals
426 are not as dorsoventrally low as in *Plesiochelys etalloni* (Paulina-Carabajal et al. 2013), meiolaniids

427 (Paulina-Carabajal et al. 2017), and some other cryptodires (e.g. *Chelonoidis nigra*, *Chelonoidis chilensis*,
428 *Trachemys scripta*, and *Carettochelys insculpta*; Georgi and Sipla 2008; Paulina-Carabajal et al. 2017),
429 but more elevated as in *Gopherus berlandieri*, *Chelydra serpentina* and *Malacochersus tornieri* (Walsh et
430 al. 2009; Mautner et al. 2017; Paulina-Carabajal et al. 2017). The vertical canals (ASC and PSC) are
431 elongated in the anteroposterior axis (Fig. 4), which could indicate an aquatic behaviour according to
432 Georgi and Sipla (2008). As in *Plesiochelys etalloni* and most known turtles (Paulina-Carabajal et al.
433 2013, 2017), the crus communis is located at the midline of the vestibular organ (Fig. 4). The angle
434 formed between the ASC and the PSC is 87.8°, wider than that described for *Plesiochelys etalloni* or
435 *Trachemys scripta* (Paulina-Carabajal et al. 2013), but lower than that of any terrestrial taxa (Paulina-
436 Carabajal et al. 2017). The lateral semicircular canal (LSC) is the thickest (1.1 mm) of the three, as in
437 *Plesiochelys etalloni*, followed by the ASC (0.8 mm) and the PSC (0.6 mm). The ASC is slightly more
438 elongated than the PSC (2.2 mm and 2.1 mm, respectively). As in *Plesiochelys etalloni* (Paulina-
439 Carabajal et al. 2013), the anterior ampulla is well developed whereas the posterior is much slender (Fig.
440 4e), in contrast to that of several testudinids (Paulina-Carabajal et al. 2017).

441 The lagena in *The new taxon* is well-developed ventrally (Fig. 4d), similarly to those of
442 *Plesiochelys etalloni*, *Gopherus berlandieri*, and *Testudo hermanni*, in contrast to those of *Rhinoclemmys*
443 *funerea* and *Kinixys belliana* (Paulina-Carabajal et al. 2013, 2017), in which this region is more rounded.
444 The fenestra ovalis is smaller than that of *Malacochersus tornieri* (Mautner et al. 2017). The columella
445 auris is preserved on both sides (Fig. 4), except for the distal portion. Its shaft is thinner than in
446 *Plesiochelys etalloni*, and projects anterolaterally, in contrast to the posterolaterally projection of the latter
447 (Paulina-Carabajal et al. 2013). The foot plate is broad and concave medially, towards the fenestra ovalis.

448

449 **Podocnemidoidea** Broin, 1988

450 ***Roxochelys*** Price, 1953

451 *Type species. Roxochelys wanderleyi* Price, 1953.

452 *Diagnosis (emended).* A medium-size Podocnemidoidea (more than 300 mm of carapace length) with a
453 shell surface with fine sculpturing composed of small polygons; vertebral scutes 2-4 hexagonal and
454 narrower than the pleural scutes; a relatively short and wide nuchal bone (in comparison to other non-
455 Podocnemididae Podocnemidoidea), with a wide anterior edge; four-sided first neural bone; axillary
456 buttress extending onto costal bones 2 and reaching the peripheral bones 3 anteriorly; suture for axillary

457 buttress medially broad and laterally narrow; costal bones 2 thickened around the axillary buttress suture;
458 bridge peripheral bones unguittered; iliac scar on costal bone 7 with concave anterior outline that crosses
459 from costal bone 8 onto costal bone 7 both medially and laterally; internal gutter of posterior peripheral
460 bones and pygal bone absent; gular scutes restricted to the epiplastra; intergular scute relatively wide;
461 long midline contact between humeral scutes; pectoral scutes reach the entoplastron but not the epiplastra
462 or mesoplastra.

463 *Roxochelys wanderleyi* Price, 1953

464 Figure 5

465 *Holotype*. MCT (DGM) 216-R housed at Museu de Ciências da Terra, Rio de Janeiro, Brazil.

466 *Diagnosis*. Same as for genus.

467 *Studied material*. MPMA-10-0003/03 (Fig. 5) an almost complete, but heavily crushed and partially
468 disarticulated shell.

469 *Locality and Horizon*. A reddish sandstone of the Late Cretaceous Adamantina Formation, exposed near
470 the urban area of Monte Alto, São Paulo, Brazil (S 21° 14' 03,6", W 48° 30' 27,5") (Fig. 1).

471 *Description*. MPMA-10-0003/03 consists of a large (approximately 50 cm long) partially articulated, but
472 very cracked and crushed shell (Fig. 5), preventing the analysis of its visceral structures. The right costal
473 plate 7, both costal plates 8, the suprapygial, pygal, and some peripheral plates are not preserved. Some of
474 the scute sulci are seen on the carapace, allowing a partial reconstruction of the scute pattern (Fig. 5b). All
475 the plastral bones are preserved, except for parts of the right epiplastron and xiphiplastron. The ventral
476 surface of the plastron is somewhat eroded, preventing the identification of scute sulci (Fig. 5d). The
477 typical ornamentation of braided lines and small polygons found in the outer surface of *Roxochelys*
478 *wanderleyi* shells (Broin 1971, 1991; Gaffney et al. 2011) is also seen in the carapace of MPMA-10-
479 0003/03 (Fig. 5a). However, similar ornamentation patterns can also be found in some non-
480 Podocnemidoid taxa (e.g., the different species of *Hydromedusa*) and some extant podocnemidids (e.g.
481 *Peltocephalus dumerilianus* and the different species of *Podocnemis*; pers. comm. E. Cadena), and may
482 not be a reliable feature to identify turtle taxa.

483 Only a partial contour of the left edge of the nuchal bone can be seen (Fig. 5a, b). It reveals a
484 relatively broad plate without an anterior narrowing margin, as in other specimens referred to *Roxochelys*
485 *wanderleyi* (Price 1953; Romano et al. 2013), and differing from other taxa found in the Bauru Basin
486 (Gaffney et al. 2011). The neural series is partially preserved (the fifth element missing). The neural bone

487 1 is four-sided, not contacting the costal bones 2 (Fig. 5b). This is seen in *R. wanderleyi* (Price 1953;
488 Romano et al. 2013) and *Cambaremys langertoni* (França & Langer 2005), but not in *Bauruemys elegans*,
489 the four-sided neural plate of which is the second (Suárez 1969; Kischlat 1994; Romano and Azevedo
490 2007; Gaffney et al. 2011; Romano et al. 2013). The last preserved neural bone is the hexagonal sixth
491 plate. Usually the last neural plate of a complete series is pentagonal or heptagonal in shape, due to the
492 converging posterior contact with the costal plates. Thus, the last neural plate is probably missing from
493 MPMA-10-0003/03, which would have a neural series composed of seven bones (Fig. 5a, b). Intraspecific
494 variation in the length of the neural series is not uncommon within podocnemidoids and *R. wanderleyi* are
495 known from specimens with six and seven plates (Gaffney et al. 2011; Romano et al. 2013).

496 The scute pattern is the same as in all so far known specimens of *Roxochelys wanderleyi* (Price,
497 1953; Gaffney et al. 2011; Romano et al. 2013). The marginal scutes 1 are antero-posteriorly short, but
498 their lateral limits are not preserved, so that their total width is unclear. The vertebral 1 is medio-laterally
499 shorter than vertebral scutes 2 and 3 (Fig. 5a, b), and these are hexagonal in shape (sulci are only partially
500 preserved in vertebral 4). The pleural scutes are wider than the vertebral scutes. As in *Bauruemys elegans*
501 (Suárez 1969) and other *Roxochelys wanderleyi* specimens (Gaffney et al. 2011; Romano et al. 2013), the
502 pleuromarginal sulci of MPMA-10-0003/03 are restricted to the lateral third of the peripheral bones
503 (Gaffney et al. 2011; Romano et al. 2013). However, the characteristic guttering in the marginal scutes of
504 *B. elegans* (Gaffney et al. 2011) is absent in MPMA-10-0003/03.

505 The plastron of MPMA-10-0003/03 shows the common Podocnemidoidae morphology (Fig. 5c),
506 seen in all Bauru Basin taxa. The entoplastron is diamond-shaped and contacts the epiplastra anteriorly
507 and the hyoplastra posteriorly. The mesoplastron is rounded and located laterally, sutured to the
508 hyoplastron anteriorly, peripherals 5 and 6 laterally, and the hypoplastron posteriorly (Fig. 5c, d). The
509 pectoroabdominal sulcus apparently does not cross the mesoplastron, as in MCT 1787-R, referred to
510 *Roxochelys wanderleyi*. However, this region is poorly preserved in MPMA-10-0003/03 and the
511 identification of this sulcus is not clear (Fig. 5c, d).

512

513 **Additional specimens**

514 Three more fragmentary specimens (Fig. 6) have been found in the same locality as MPMA 04-
515 0008/89. The more complete of these, MPMA 04-0009/89, is composed of several carapace fragments,
516 including costal and peripheral plates. MPMA 04-0014/89 is an articulated carapace fragment, including

517 three partially preserved left costal plates and two neural plates. Neither of them possess diagnostic
518 features of any particular subclade and are hence considered Testudines indet. MPMA 04-0017/89 is
519 represented by a costal bone, a left hyoplastron fragment, and a pelvic girdle fragment, including mostly
520 parts of the ilium, but also fragments of the ischium, and pubis, and can be assigned to Pleurodira. The
521 latter is comparable in relative size to MPMA 04-0008/89, but those were not found closely associated
522 and, hence, we refrain from referring them to the same specimen. The two other specimens are somewhat
523 larger. The peripheral plates of MPMA 04-0014/89 bear the same reticulation pattern found in MPMA-
524 10-0003/03.

525

526 **Discussion**

527

528 Our phylogenetic analysis found six most parsimonious trees (MPTs) with 238 steps each (see
529 Supplementary Data). The MPTs differ in the relative position of some outgroup taxa (i.e., *Araripemys*
530 *barretoii*, Pelomedusidae), as well as *Hamadachelys escuilliei* and *Portezueloemys patagoinica*, and some
531 species of *Podocnemis*. All most parsimonious trees (Fig. 6; Supplementary Data) shows *The new taxon*
532 nested within Peiopemydodda, in a polytomy including *Peiopemys mezzalirai* and the clade formed by
533 *Pricemys caiera* and *Lapparentemys vilavilensis*. Peiopemydodda is supported by an anteroventral
534 emargination reaching above the ventral level of the orbit (ch. 13, state 2). The scoring of *The new taxon*
535 in the data matrix differs from that of *Peiopemys mezzalirai* by two conditions: the foramen palatinum
536 posterius on the palatine-pterygoid suture, rather than restricted to the palatine (ch. 37) and a larger
537 antrum postoticum (ch. 40). The size of the antrum postoticum also sets the taxon apart from *Pricemys*
538 *caiera* and *Lapparentemys vilavilensis*. The larger foramen nervi abducentis (ch. 65) of the former and the
539 shallow fossa precolumellaris (ch. 41) of the latter also differentiate those peiopemydods from *The new*
540 *taxon*. Those distinct features, associated with its smaller size and stratigraphic provenance further
541 supports the assignment of MPMA 04-0008/89 to a distinct peiopemydod taxon. As such, it extends the
542 record of Peiopemydodda to pre-Maastrichtian times (Fig. 7), with the clade surviving until the early
543 Paleocene (Broin 1971, 1991; Gaffney et al. 2011).

544 Although some authors used Computed Tomography to study osteological traits (e.g. Brinkman
545 et al. 2006; Lipka et al. 2006; Sterli et al. 2010; Cadena and Jaramillo 2015; Lively 2015) of extinct
546 turtles, only four other studies were published so far with digital reconstructions of their soft tissue organs

547 (Georgi and Sipla 2008; Paulina-Carabajal et al. 2013, 2017; Mautner et al. 2017). Indeed, this is the first
548 study to employ these tools to assess the inner ear and neuroanatomy of an extinct pleurodire. The
549 endocast and inner ear of *The new taxon* are similar to those of other turtles. However, some differences
550 are noted, such as the position of the medulla oblongata almost on the same level as the cerebral
551 hemispheres (Fig. 4a), whereas the condition in the bothremydids *Bothremys cooki* and *Chedighaii*
552 *barberi* (Hopson 1979) resembles that of sea turtles (Wyneken 2001), in which the medulla oblongata is
553 located well below the cerebral hemispheres, with stronger pontine and cephalic flexures. Those
554 differences could be related to the adaptations of bothremydids to marine environments, as suggested by
555 some authors (e.g. Gaffney et al. 2006; Rabi et al. 2012; Joyce et al. 2016). However, with such a small
556 sample, especially for pleurodires, it is premature to infer phylogenetic or behavioural trends from the
557 neuroanatomy of fossil turtles. Future, more comprehensive studies may employ the data presented here
558 to better explore the evolution of those organs in Pleurodira and Testudines. We also provided a detailed
559 account of the cranial nerves and arteries in *The new taxon*. As noted above, the patterns of carotid
560 circulation in turtles has been mainly studied in stem-turtles and cryptodires. Given that several
561 phylogenetic characters are related to the circulatory and nerve systems, such as skull foramina and canals
562 (e.g. Joyce 2007; Sterli et al. 2010; Müller et al. 2011; Gaffney et al. 2006, 2011; Rabi et al. 2013), our
563 study adds new data to understand the patterns in Pleurodira.

564 The assignment of MPMA-10-0003/03 to *Roxochelys wanderleyi* is based on the general
565 podocnemidoid morphology of the shell, the four-sided neural plate 1, the broad nuchal plate, and the
566 reticulation pattern of ornamentation on its external surface (Broin 1991; Gaffney et al. 2011; Romano et
567 al. 2013). *Roxochelys wanderleyi* was previously recorded in the Adamantina Formation from the type-
568 locality in Mirandópolis, as well as in the area of Presidente Prudente, both in São Paulo, Brazil (Price
569 1953; Broin 1971; Gaffney et al. 2011; Romano et al. 2013; Menegazzo et al. 2015). The new specimen
570 extends the putative record of this taxon to another Adamantina Formation site. In addition, most of the
571 specimens so far referred to *R. wanderleyi* are smaller than 50 cm of carapace length (Romano et al.
572 2013), so that the new specimen represents one of the largest yet attributed to the taxon.

573

574 **Conclusions**

575

576 A partial skull from the Late Cretaceous Adamantina Formation represents the first extinct pleurodire and
577 one of the few fossil turtles to have its neuroanatomy described based on digitally reconstructed endocast
578 and inner ear. The large antrum postoticum and fossa precolumellaris, the foramen prepalatinum formed
579 by the pterygoid and palatine, and the triangular dermal scute vii with an anterior notch on the midline, as
580 well as its smaller size and distinct stratigraphic provenance, support the assignment of this specimen to a
581 new taxon, *The new taxon*, placed inside Peiropemydodda in our phylogenetic analysis . This fossil
582 extends the range of that clade to pre-Maastrichtian times. Other fossil turtles from the Monte Alto area
583 include a new *Roxochelys wanderleyi* shell recovered from a different site of the Adamantina Formation,
584 which represents one of the largest specimens referable to that taxon.

585

586 **References**

- 587 Alvarenga, H., and W. R. Nava. 2005. Aves Enantiornithes do Cretáceo Superior da Formação
588 Adamantina do Estado de São Paulo, Brasil. *Congresso Latinoamericano de Paleontologia de*
589 *Vertebrados* 2:20. (in Portuguese)
- 590 Andrade, M. B., and R. J. Bertini. 2008. A new *Sphagesaurus* (Mesoeucrocodylia: Notosuchia) from the
591 Upper Cretaceous of Monte Alto City (Bauru Basin, Brazil), and a revision of the Sphagesauridae.
592 *Historical Biology* 20: 101 –136.
- 593 Báez, A. M., R. O. Gómez, L. C. B. Ribeiro, A. G. Martinelli, V. P. A. Teixeira, and M. L. F. Ferraz. 2012.
594 The diverse Cretaceous neobatrachian fauna of South America: *Uberabatrachus carvalhoi*, a new
595 frog from the Maastrichtian Marília Formation, Minas Gerais, Brazil. *Gondwana Research* 22:
596 1141 –1150.
- 597 Batezelli, A. 2015. Continental systems tracts of the Brazilian Cretaceous Bauru Basin and their
598 relationship with the tectonic and climatic evolution of South America. *Basin Research* 1 –25.
- 599 Bertini, R. J., L. G. Marshall, M. Gayet, and P. M. Brito. 1993. Vertebrate faunas from the Adamantina
600 and Marília (Upper Bauru Group, Late Cretaceous, Brazil) in their stratigraphic and
601 paleobiogeographic context. *Neues Jahrbuch für Geologie und Paläontologie, Monatshefte* 188:
602 71 –101.
- 603 Bertini, R. J., R. M. Santucci, and A. C. Arruda-Campos. 2001. Titanossauros (Sauropoda: Saurischia) no
604 Cretáceo Superior continental (Formação Marília, Membro Echaporã) de Monte Alto, estado de

605 São Paulo, e correlação com formas associadas do Triângulo Mineiro. *Geociências* 20(1): 93–103.
606 (in Portuguese)

607 Bittencourt, J. S., and M. C. Langer. 2011. Mesozoic dinosaurs from Brazil and their biogeographic
608 implications. *Anais da Academia Brasileira de Ciências* 83: 23–60.

609 Brinkman, D., M. Hart, H. Jamniczky, and M. Colbert. 2006. *Nichollsemys baieri* gen. et sp. nov., a
610 primitive chelonioid turtle from the Late Campanian of North America. *Paludicol* 5(4): 111–124.

611 Brito, R. J., C. R. L. Amaral, and L. P. Machado. 2006. A ictiofauna do Grupo Bauru, Cretáceo Superior
612 da Bacia Bauru, Sudeste do Brasil. In *Paleontologia de Vertebrados: Grandes Temas e*
613 *Contribuições Científicas*, eds. V. Gallo, P. M. Brito, H. M. Silva, and F. J. Figueroa, 133–143. Rio
614 de Janeiro: Editora Interciência. (in Portuguese)

615 Broin, F. de. 1971. Une espèce nouvelle de tortue pleurodire (? *Roxochelys vilavilensis* n. sp.) dans le
616 Crétacé supérieur de Bolivie. *Bulletin de la Société Géologique de France* 7(3–4): 445–452. (in
617 French)

618 Broin, F. de. 1991. Fossil turtles from Bolivia. In *Fosiles y Facies de Bolivia, Volume 1. Vertebrados*, ed.
619 R. Suarez-Soruco, 509–527. Revista Técnica de Yacimientos Petrolíferos Fiscales de Bolivia, 12.

620 Cadena, E. 2015. A global phylogeny of Pelomedusoides turtles with new material of *Neochelys franzeni*
621 Schleich, 1993 (Testudines, Podocnemididae) from the middle Eocene, Messel Pit, of Germany.
622 *PeerJ* 3:e1221. doi:10.7717/peerj.1221

623 Cadena, E.A., and C.A. Jaramillo. 2015. The first fossil skull of *Chelus* (Pleurodira: Chelidae, Matamata
624 turtle) from the early Miocene of Colombia. *Palaeontologia Electronica* 18.2.32A: 1–10.

625 Cadena, E. A., D. T. Ksepka, C. A. Jaramillo, and J. I. Bloch. 2012. New pelomedusoid turtles from the
626 late Palaeocene Cerrejón Formation of Colombia and their implications for phylogeny and body
627 size evolution. *Journal of Systematic Palaeontology* 10(2): 313–331.

628 Carvalho, I. S., F. M. Vasconcellos, and S. A. S. Tavares. 2007. *Montealtosuchus arrudacamposi*, a new
629 peirosaurid crocodile (Mesoeucrocodylia) from the Late Cretaceous Adamantina Formation of
630 Brazil. *Zootaxa* 1607: 35–46.

631 Cope, E. D. 1864. On the limits and relations of the Raniformes. *Proceedings of the Academy of Natural*
632 *Sciences of Philadelphia* 1864: 181–183.

633 Cope, E. D. 1868. On the origin of genera. *Proceedings of the Academy of Natural Sciences of*
634 *Philadelphia* 1868: 242–300.

635 de la Fuente, M. S. 2003. Two new pleurodiran turtles from the Portezuelo Formation (Upper Cretaceous)
636 of Northern Patagonia, Argentina. *Journal of Paleontology* 77(3): 559–575.

637 Dumont Junior, M. V. 2013. Um novo podocnemídeo fóssil de grande porte da Formação Solimões
638 (Mioceno-Plioceno), Acre, Brasil e as relações filogenéticas entre os Podocnemidae. *Unpublished*
639 *M.S. thesis, Universidade de Brasília, 1–67. Brasília, Brazil.* (in Portuguese)

640 Fachini, T. S., and A. S. Hsiou. 2011. Presence of an “anilioid” snake from the Late Cretaceous of
641 Adamantina Formation, Brazil. 4th Congreso Latinoamericano de Paleontología de Vertebrados
642 13.

643 Fachini, T. S., and F. V. Iori. 2009. Primeiro registro fóssil de Squamata na região do município de Monte
644 Alto, estado de São Paulo (Bacia Bauru, Cretáceo Superior). XXI Congresso Brasileiro de
645 Paleontologia 172. (in Portuguese)

646 Fernandes, L. A., and A. M. Coimbra. 1996. A Bacia Bauru (Cretaceo Superior, Brasil). *Anais da*
647 *Academia Brasileira de Ciencias* 68(2): 195– 205. (in Portuguese)

648 Ferreira, G. S., A. D. Rincón, A. Solórzano, and M. C. Langer. 2015. The last marine pelomedusoids
649 (Testudines: Pleurodira): a new species of *Bairdemys* and the paleoecology of *Stereogenyina*.
650 *PeerJ* 3: e1063.

651 França, M. A. G., and M. C. Langer. 2005. A new freshwater turtle (Reptilia, Pleurodira, Podocnemidae)
652 from the Upper cretaceous (Maastrichtian) of Minas Gerais, Brazil. *Geodiversitas* 27(3): 391–411.

653 França, M. A. G., and M. C. Langer. 2006. Phylogenetic relationships of the Bauru Group turtles (Late
654 Cretaceous of south-central Brazil). *Revista Brasileira de Paleontologia* 9(3): 365–373.

655 Gaffney, E.S. 1977. An endocranial cast of the side-necked turtle, *Bothremys*, with a new reconstruction
656 of the palate. *American Museum Novitates* 2639: 1–12.

657 Gaffney, E. S. 1979. Comparative cranial morphology of recent and fossil turtles. *Bulletin of the*
658 *American Museum of Natural History* 164(2): 65–376.

659 Gaffney, E.S. 1982. Cranial morphology of the baenid turtles. *American Museum Novitates* 2737: 1–22.

660 Gaffney, E. S., P. A. Meylan, R. C. Wood, E. Simons, and D. A. Campos. 2011. Evolution of the side-
661 necked turtles: the family Podocnemididae. *Bulletin of the American Museum of Natural History*
662 350: 1–237.

- 663 Gaffney, E. S., H. Tong, and P. A. Meylan. 2006. Evolution of the side-necked turtles: the families
664 Bothremydidae, Euraxemydidae, and Araripemydidae. *Bulletin of the American Museum of*
665 *Natural History* 300: 1–698.
- 666 Gaffney, E.S., and R. Zangerl. 1968. A revision of the chelonian genus Bothremys (Pleurodira:
667 Pelomedusidae). *Fieldiana Geologica* 16: 193–239.
- 668 Georgi, J.A., and J.S. Sipla. 2008. Comparative and functional anatomy of balance in aquatic reptiles and
669 birds. In *Sensory Evolution on Threshold: Adaptations on Secondarily Aquatic Vertebrates*, eds.
670 J.G.M. Thewissen, and S. Nummela, 233–256. Berkeley, California: University of California Press.
- 671 Goloboff, P. A., J. S. Farris, M. Kallérjö, B. Oxelman, M. Ramírez, and C. Szumik. 2003. Improvements
672 to resampling measures of group support. *Cladistics* 19: 324–332.
- 673 Goloboff, P. A., J. S. Farris, and K. C. Nixon. 2008. TNT, a free-program for phylogenetic analysis.
674 *Cladistics* 24: 774–786.
- 675 Hermanson, G., G. S. Ferreira, and M. C. Langer. 2016. The largest Cretaceous podocnemidoid turtle
676 (Pleurodira) revealed by an isolated plate from the Bauru Basin, south-central Brazil. *Historical*
677 *Biology* 29(6): 833–840. doi: 10.1080/08912963.2016.1248434
- 678 Hopson JA. 1979. Paleoneurology. In *Biology of the Reptilia*, vol. 9, ed. C. Gans, 39–146. New York:
679 Academic Press.
- 680 Iori, F. V., and I. S. Carvalho. 2009. *Morrinhosuchus luziae*, um novo Crocodylomorpha Notosuchia da
681 Bacia Bauru, Brasil. *Revista Brasileira de Geociências* 39: 717–725.
- 682 Iori, F. V., and I. S. Carvalho. 2010. Ocorrência de um quelônio de grande porte no município de Monte
683 Alto, estado de São Paulo, Brasil (Bacia Bauru, Cretáceo Superior). VII Simpósio Brasileiro de
684 Paleontologia de Vertebrados 44. (in Portuguese)
- 685 Iori, F. V., and I. S. Carvalho. 2011. *Caipirasuchus paulistanus*, a new sphagesaurid (Crocodylomorpha,
686 Mesoeucrocodylia) from the Adamantina Formation (Upper Cretaceous, Turonian-Santonian),
687 Bauru Basin, Brazil. *Journal of Vertebrate Paleontology* 31: 1255–1264.
- 688 Iori, F. V., and K. L. Garcia. 2012. *Barreirosuchus franciscoi*, um novo Crocodylomorpha
689 Trematochampsidae da Bacia Bauru, Brasil. *Revista Brasileira de Geociências* 42: 397–410.
- 690 Joyce, W. G. 2007. Phylogenetic relationships of Mesozoic Turtles. *Bulletin of the Peabody Museum of*
691 *Natural History* 48: 3–102.

692 Joyce, W.G., T.R. Lyson, and J.I. Kirkland. 2016. An early bothremydid (Testudines, Pleurodira) from the
693 Late Cenomanian of Utah, North America. *PeerJ* 4: e2502.

694 Kischlat, E.-E. 1994. Observações sobre *Podocnemis elegans* Suarez (Chelonii, Pleurodira,
695 Podocnemididae) do Neocreatáceo do Brasil. *Acta Geologica Leopoldensia* 17: 345–351. (in
696 Portuguese)

697 Kischlat, E.-E. 2015. A new pleurodire turtle (Chelonii) from Adamantina Formation (Bauru Group),
698 Upper Cretaceous of Brazil. *PeerJ Preprints* 3: e1075

699 Kischlat, E. E., and S. A. K. Azevedo. 1991. Sobre novos restos de quelônios podocnemídeos do Grupo
700 Bauru, estado de São Paulo, Brasil. XII Congresso Brasileiro de Paleontologia 12:25–26. (in
701 Portuguese)

702 Lapparent de Broin, F. 2000. The oldest prepodocnemidid turtle (Chelonii, Pleurodira), from the Early
703 Cretaceous, Ceará State, Brasil, and its environment. *Treballs del Museu de Geologia de*
704 *Barcelona* 9: 43–95.

705 Lipka, T.R., F. Therrien, D.B. Weishampel, H.A. Jamniczky, W.G. Joyce, M.W. Colbert, and D.B.
706 Brinkman. 2006. A new turtle from the Arundel clay facies (Potomac Formation, Early
707 Cretaceous) of Maryland, U.S.A. *Journal of Vertebrate Paleontology* 26(2): 300–307.

708 Lively, J.R. 2015. A new species of baenid turtle from the Kaiparowits Formation (Upper Cretaceous,
709 Campanian) of southern Utah. *Journal of Vertebrate Paleontology* e1009084.
710 doi:10.1080/02724634.2015.1009084

711 Martinelli, A. G., and W. R. Nava. 2011. A new squamate lizard from the Upper Cretaceous Adamantina
712 Formation (Bauru Group), São Paulo State, Brazil. *Anais da Academia Brasileira de Ciências* 83:
713 291–299.

714 Mautner, A.-K., A.E. Latimer, U. Fritz, and T.M. Scheyer. 2017. An updated description of the osteology
715 of the pancake tortoise *Malacochersus tornieri* (Testudines: Testudinidae) with special focus on
716 intraspecific variation. *Journal of Morphology*. doi:10.1002/jmor.20640

717 Méndez, A. H., F. E. Novas, and F. V. Iori. 2014. New record of abelisauroid theropods from the Bauru
718 Group (Upper Cretaceous), São Paulo State, Brazil. *Revista Brasileira de Paleontologia* 17(1): 23–
719 32.

- 720 Menegazzo, M. C., R. J. Bertini, and F. F. Manzini. 2015. A new turtle from the Upper Cretaceous Bauru
721 Group of Brazil, updated phylogeny and implications for age of the Santo Anastácio Formation.
722 *Journal of South American Earth Sciences* 58: 18–32.
- 723 Menegazzo, M. C., O. Catuneanu, and H. K. Chang. 2016. The South American retroarc foreland system:
724 the development of the Bauru Basin in the back-bulge province. *Marine and Petroleum Geology*.
725 73: 131–156.
- 726 Meylan, P. A., E. S. Gaffney, and D. A. Campos. 2009. *Caninemys*, a new side-necked turtle
727 (Pelomedusoides: Podocnemididae) from the Miocene of Brazil. *American Museum Novitates*
728 3639: 1–26.
- 729 Müller, J., J. Sterli, and J. Anquetin. 2011: Carotid circulation in amniotes and its implications for turtle
730 relationships. *Neues Jahrbuch für Geologie und Paläontologie* 261: 289–297.
- 731 Pacheco, J. A. 1913. Notas sobre a geologia do Vale do Rio Grande, a partir da foz do Rio Pardo até a sua
732 confluência com o Rio Paranahyba. In *Exploração do Rio Grande e de seus Afluentes*, ed. J.
733 Dourados, 33–38. São Paulo: Comissão de Geografia e Geologia. (in Portuguese)
- 734 Paulina-Carabajal, A.P., J. Sterli, J. Müller, and A. Hilger. 2013. Neuroanatomy of the marine Jurassic
735 turtle *Plesiochelys etalloni* (Testudinata, Plesiochelyidae). *PLoS ONE* 8(7): e69264.
- 736 Paulina-Carabajal, A., J. Sterli, J. Georgi, S. F. Poropat, B. P. Kear. 2017. Comparative neuroanatomy of
737 extinct horned turtles (Meiolaniidae) and extant terrestrial turtles (Testudinidae), with comments
738 on the palaeobiological implications of selected endocranial features. *Zoological Journal of the*
739 *Linnean Society* zlw024: 1–21. doi: 10.1093/zoolinnean/zlw024
- 740 Pinheiro, A. E. P., R. J. Bertini, M. A. Andrade, and R. G. Martins Neto. 2008. A new specimen of
741 *Stratiotosuchus maxhechti* (Baurusuchidae, Crocodyliformes) from the Adamantina Formation
742 (Upper Cretaceous), Southeastern Brazil. *Revista Brasileira de Paleontologia* 11(1): 37–50.
- 743 Price, L. I. 1953. Os quelônios da Formação Bauru, Cretáceo terrestre do Brasil Meridional. *Boletim da*
744 *Divisão de Geologia e Mineralogia Departamento Nacional de Produção Mineral* 147: 1–34. (in
745 Portuguese)
- 746 Rabi, M., H. Tong, and G. Botfalvai. 2012. A new species of the side-necked turtle *Foxemys*
747 (Pelomedusoides: Bothremydidae) from the Late Cretaceous of Hungary and the historical
748 biogeography of the Bothremydini. *Geological Magazine* 149: 662–674.

- 749 Rabi, M., C-F. Zhou, O. Wings, S. Ge, and W. G. Joyce. 2013. A new xinjiangchelyid turtle from the
750 Middle Jurassic of Xinjiang, China and the evolution of the basiptyergoid process in Mesozoic
751 turtles. *BMC Evolutionary Biology* 13:203. doi: 10.1186/1471-2148-13-203
- 752 Romano, P. S. R., G. R. Oliveira, S. A. K. Azevedo, A. W. A. Kellner, and D. A. Campos. 2013. New
753 information about Pelomedusoides (Testudines: Pleurodira) from the Cretaceous of Brazil. In
754 *Morphology and Evolution of Turtles (Vertebrate Paleobiology and Palaeoanthropology)*, eds. D.
755 Brinkman, P. Holroyd, and J. Gardner, 267–274. Dordrecht: Springer.
- 756 Romano, P. S. R., and S. A. K. Azevedo. 2007. Morphometric analysis of the Upper Cretaceous Brazilian
757 side-necked turtle *Bauruemys elegans* (Suárez, 1969) (Pleurodira, Podocnemididae). *Arquivos do*
758 *Museu Nacional*. 65(4): 395–402.
- 759 Santucci, R. M., and A. C. Arruda-Campos. 2011. A new sauropod (Macronaria, Titanosauria) from the
760 Adamantina Formation, Bauru Group, Upper Cretaceous of Brazil and the phylogenetic
761 relationships of Aeolosaurini. *Zootaxa* 3085: 1–33.
- 762 Staesche, K. 1937. *Podocnemis brasiliensis* n. sp. aus der Oberen Kreide Brasiliens. *Neues Jahrbuch für*
763 *Mineralogie, Geologie und Paläontologie B*, 77: 291–309. (in German)
- 764 Sterli, J., J. Müller, J. Anquetin, and A. Hilger. 2010. The parabasisphenoid complex in Mesozoic turtles
765 and the evolution of the testudinate basicranium. *Canadian Journal of Earth Sciences* 47: 1337–
766 1346.
- 767 Suárez, J. M. 1969. Um quelônio da Formação Bauru. XXIII Congresso Brasileiro de Geologia, Anais
768 3:168–176. (in Portuguese)
- 769 Tavares, S. A. S., F. R. Branco, and R. M. Santucci. 2014. Theropod teeth from the Adamantina
770 Formation (Bauru Group, Upper Cretaceous), Monte Alto, São Paulo, Brazil. *Cretaceous Research*
771 50: 59–71.
- 772 Tong, H., and E. Buffetaut. 1996. A new genus and species of pleurodiran turtle from the Cretaceous of
773 southern Morocco. *Neues Jahrbuch für Geologie und Paläontologie Abhandlungen* 199: 133–150.
- 774 Walsh, S.A., P.M. Barrett, A.C. Milner, G. Manley, and L.M. Witmer. 2009. Inner ear is a proxy for
775 deducing auditory capability and behaviour in reptiles and birds. *Proceedings of the Royal Society*
776 *B: Biological Sciences* 276: 1355–1360.
- 777 Wever, E.G. 1978. *The Reptile Ear*. Princeton, New Jersey: Princeton University Press.

- 778 Wyneken, J. 2001. *The Anatomy of Sea Turtles*. Miami: US Department of Commerce
779 NOAA Technical Memorandum NMFS-SEFSC-470.
- 780 Zangerl, R. 1960. The vertebrate fauna of the Selma Formation of Alabama. V. An
781 advanced cheloniid sea turtle. *Fieldiana: Geology Memoirs* 3(5): 281–312.

Figures

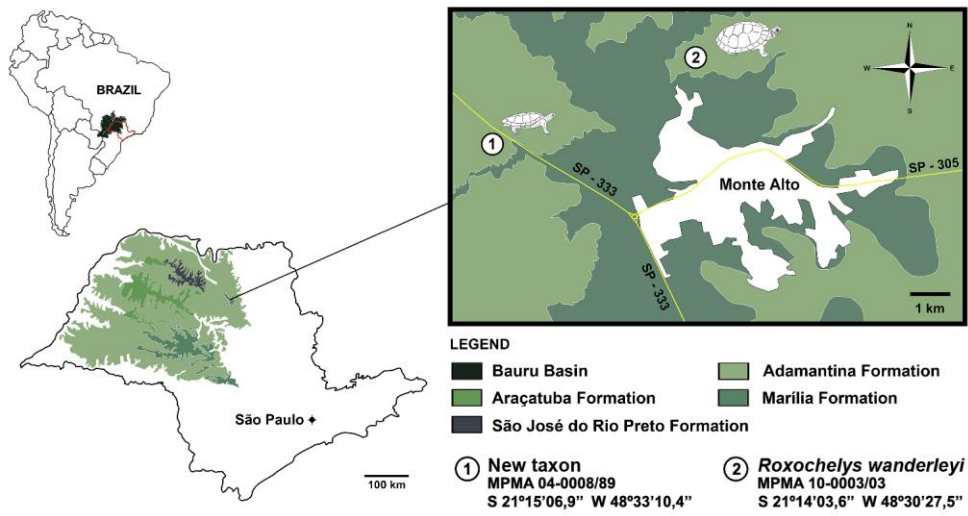


Fig.1. Location of the Bauru Basin on a South American map (top left), São Paulo state map showing the surface distribution of the stratigraphic units of the basin (bottom left), and map of the Monte Alto region highlighting the localities where the described fossils were found

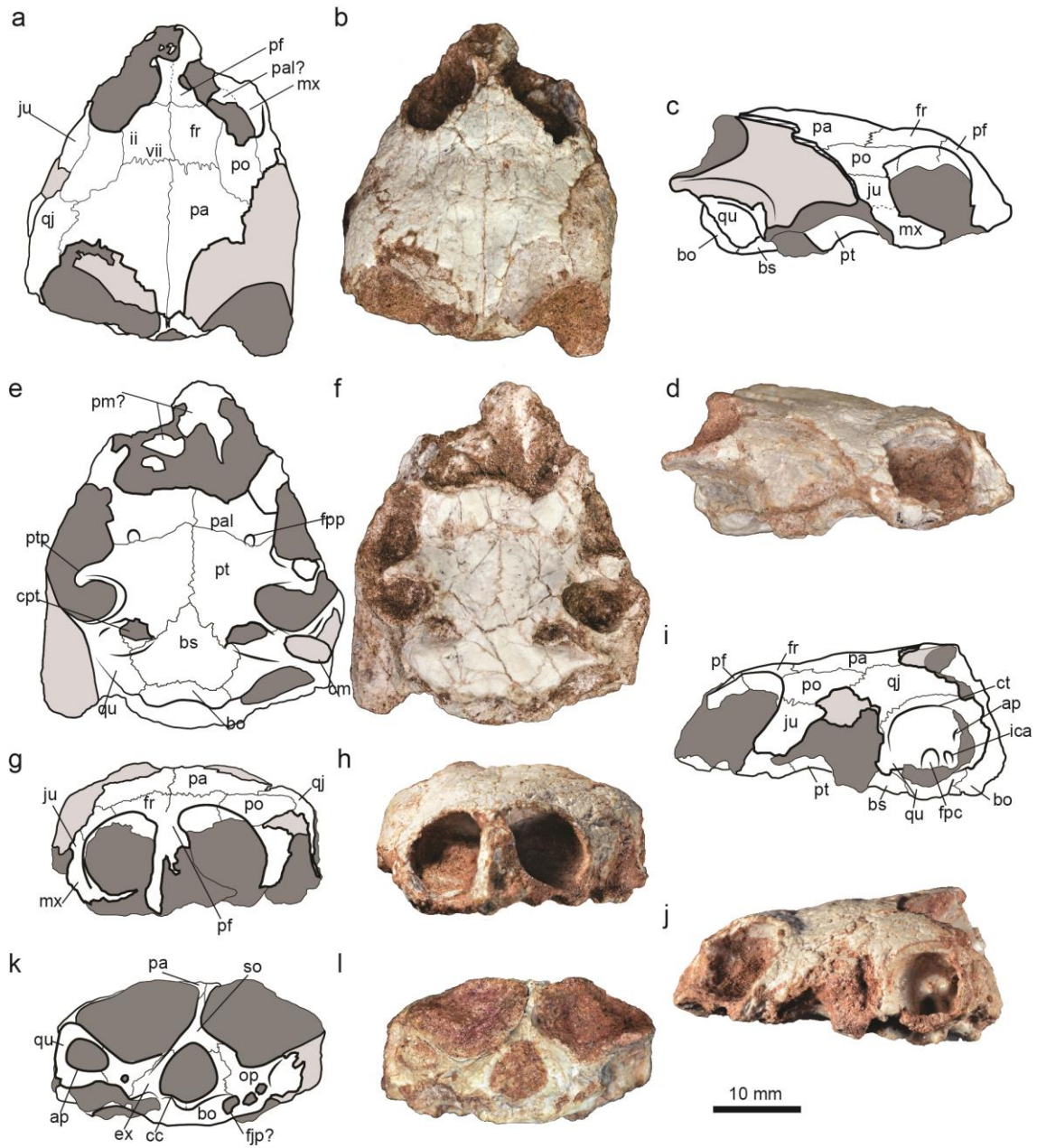


Fig. 2 *The new taxon*, MPMA 04-0008/89. Outlines and photographs of the skull in (a, b) dorsal, (c, d) right lateral, (e, f) ventral, (g, h) anterior, (i, j) left lateral, and (k, l) posterior views

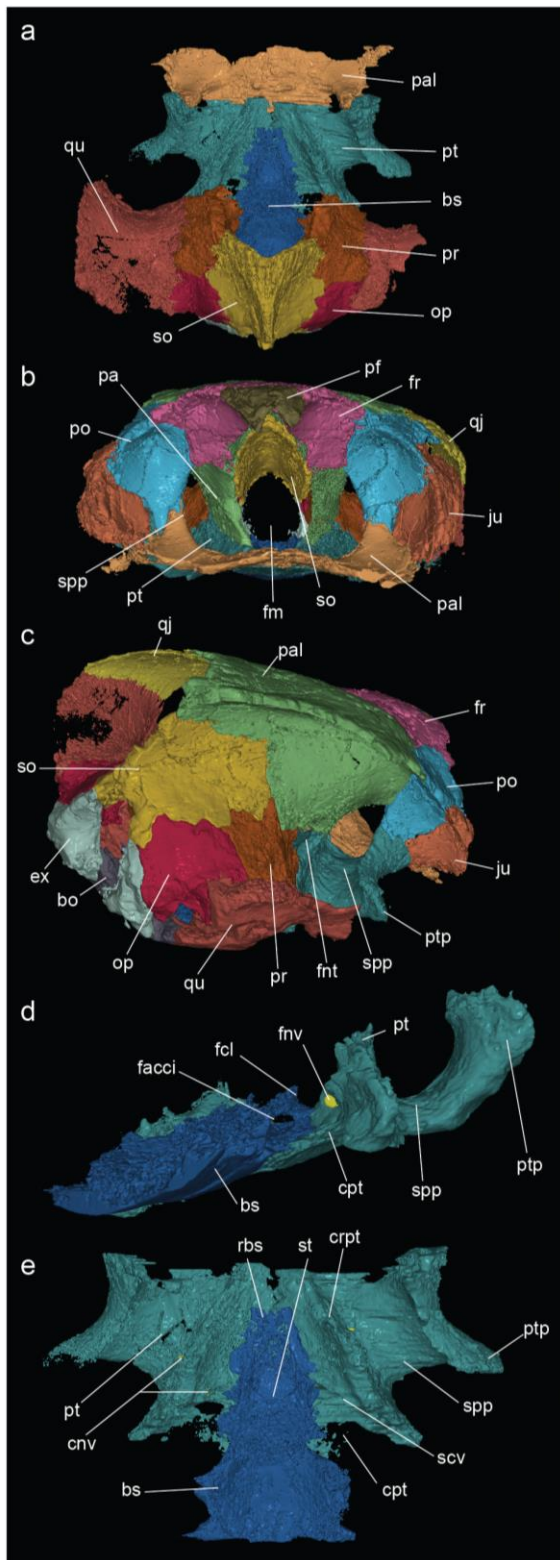


Fig. 3 *The new taxon*, MPMA 04-0008/89. Micro-CT scan reconstructed 3D models of the skull in (a) dorsal view without parietal, frontal and prefrontal bones, (b) anterior view, (c) oblique right lateral view, and isolated basisphenoid and pterygoid bones in (d) oblique left lateral and (e) dorsal views

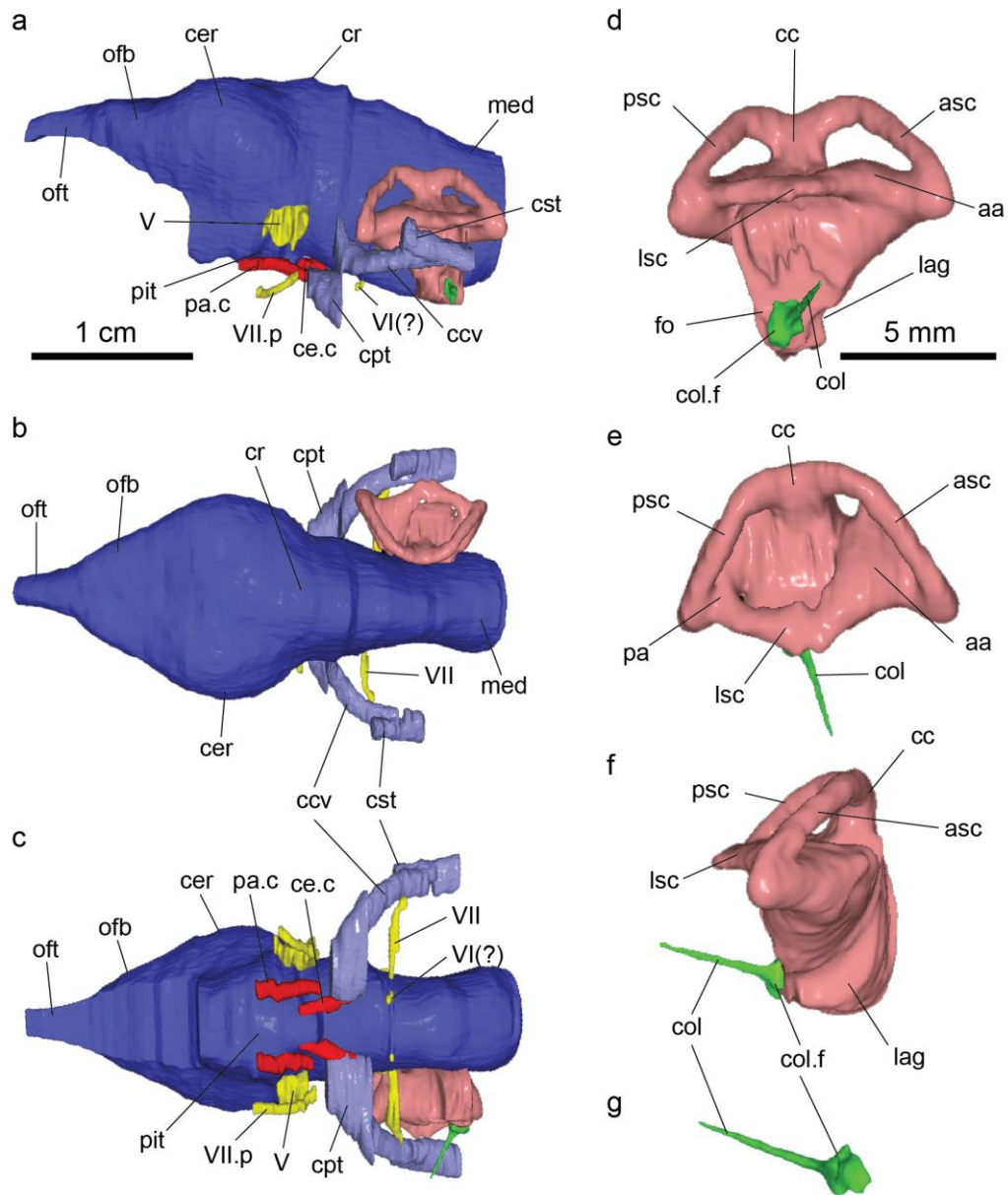


Fig. 4 *The new taxon*, MPMA 04-0008/89. Digital endocasts of the brain with associated cranial nerves and blood vessels in (a) left lateral, (b) dorsal, and (c) ventral views, and of the endosseous labyrinth with the columella auris in (d) right lateral, (e) dorsal, and (f) anterior views. On the brain endocast models only the right labyrinth is showed for better visualization.

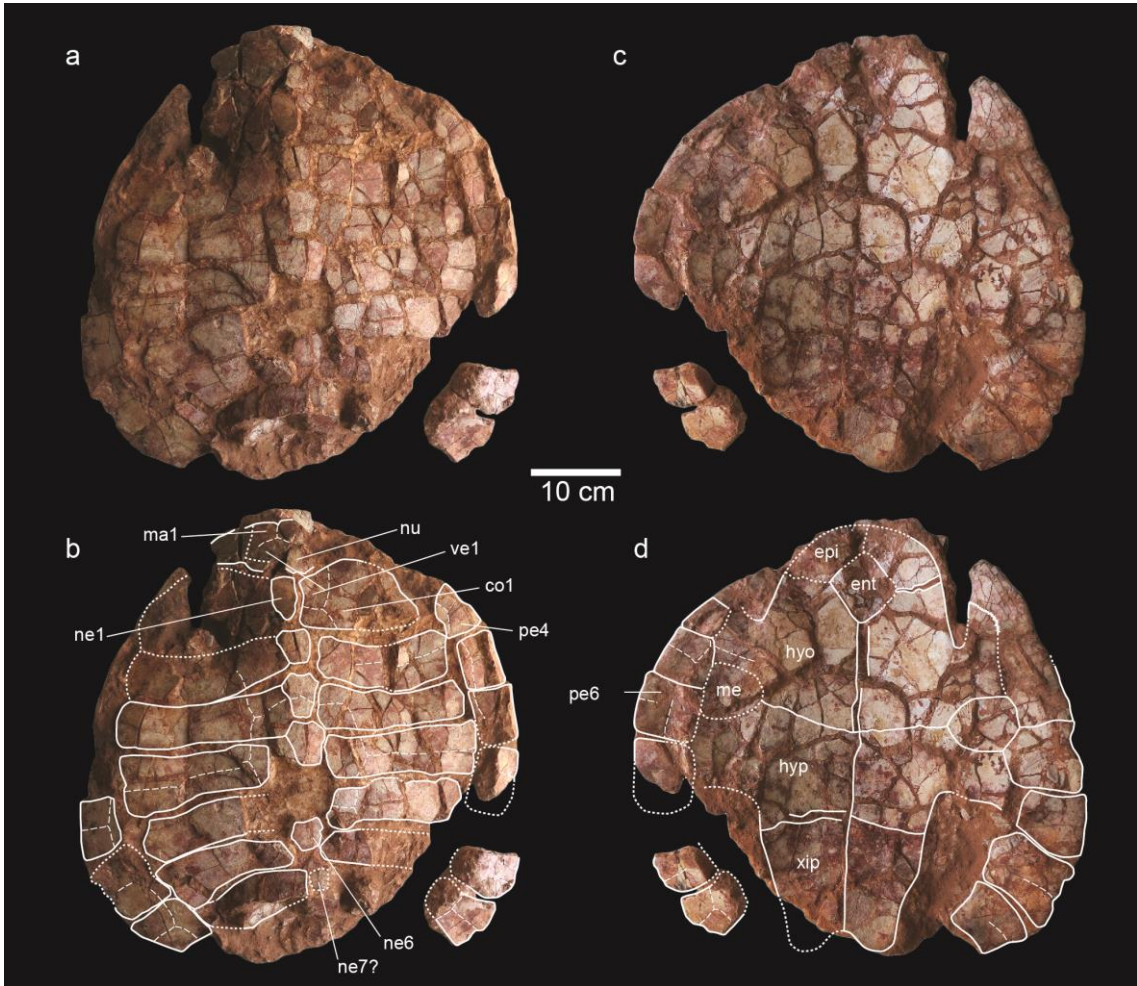


Fig. 5 *Roxochelys wanderleyi*, MPMA-10-0003/03, shell in (a-b) dorsal and (c-d) ventral views

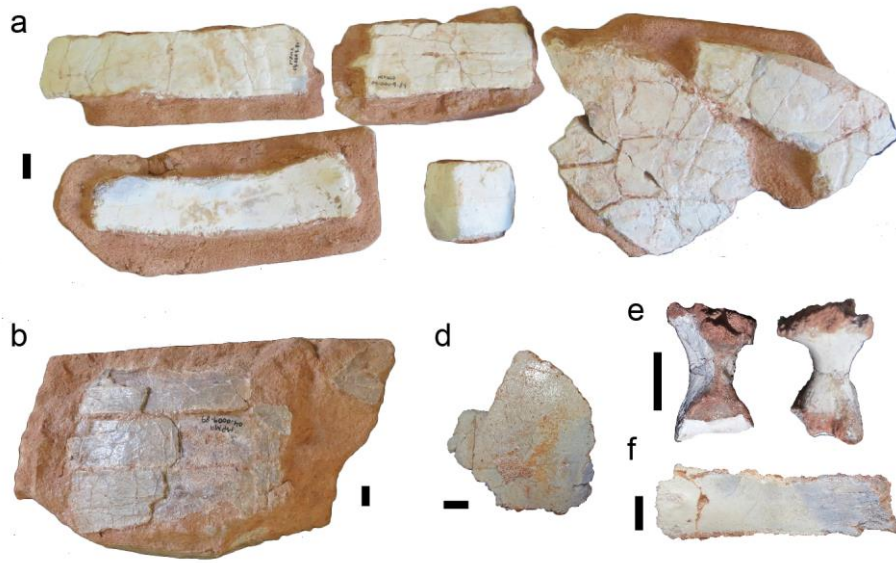


Fig. 6 Additional turtle specimens from Monte Alto, Brazil. (a) Several carapace fragments of a Testudines (MPMA 04-0009/89); (b) an articulated carapace fragment of another Testudines indet. (MPMA 04-0014/89); and fragments of (c) a left hyoplastron, (d) a pelvic girdle, and (e) a costal plate of a Pleurodira indet. (MPMA 04-0017/89). Scale bars represent 1 cm.

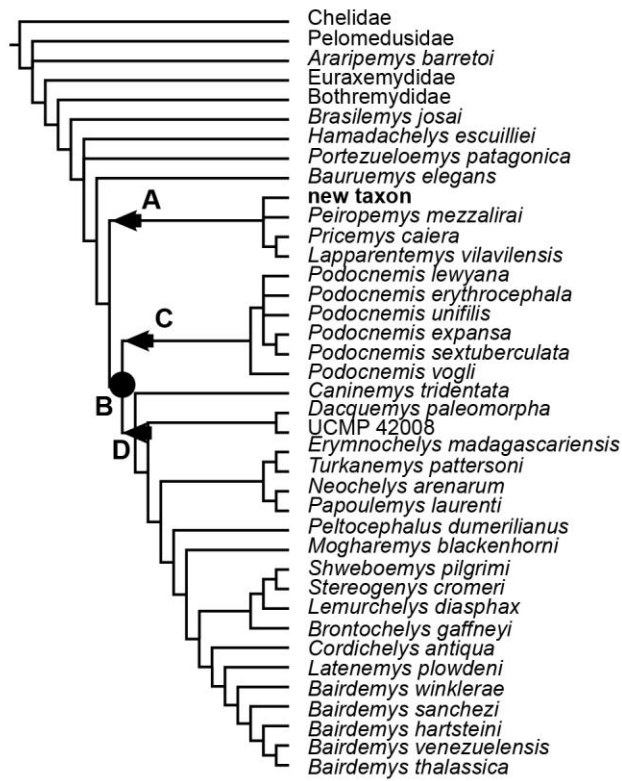


Fig. 7 Strict consensus tree resulting from the phylogenetic analysis. *The new taxon* (bold) is recovered inside the Peiropemydodda clade, along with *Peiropemys mezzalirai*, *Pricemys caiera*, and *Lapparentemys vilavilensis*. The arrows highlight the branch-based clades (A) Peiropemydodda, (C) Podocnemidinae, and (D) Erymnochelydinae, and the circle indicates the node-based clade (B) Podocnemididae.

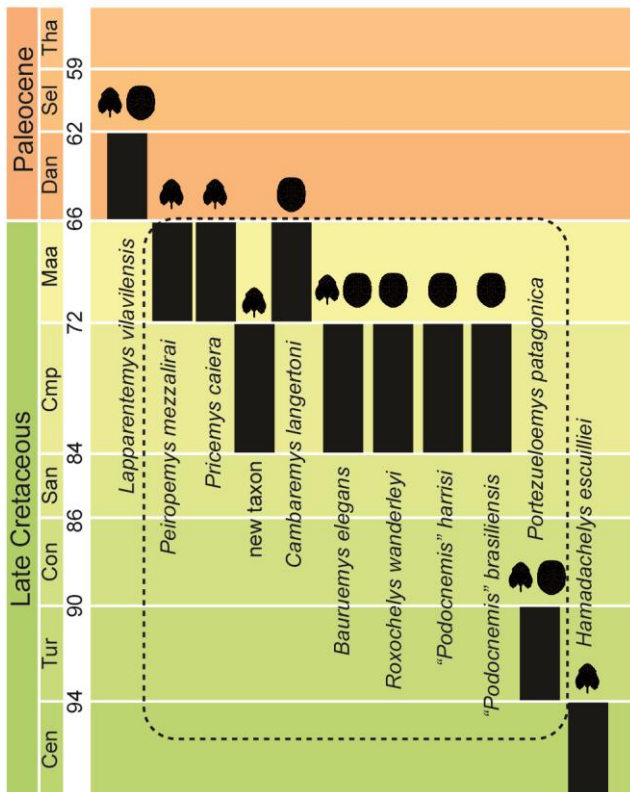


Fig. 8 Stratigraphic plot of non-Podocnemididae podocnemidoids. Black bars represent their temporal distribution; skulls and carapaces indicated the preserved skeletal parts; dotted rectangle highlights Bauru Basin taxa. Age of the Bauru Basin taxa based on Batezelli (2015)